Asymmetric behavior of charge-orbital order in electron/hole-doped *A*-site ordered manganites $Eu(Ba_{1-y}La_y)Mn_2O_6$ and $(Eu_{1-x}Ca_x)BaMn_2O_6$

D. Akahoshi,[1,*] M. Uchida,[2] T. Arima,[2,3] Y. Tomioka,[1] and Y. Tokura[1,2,4]

[1]*Correlated Electron Research Center (CERC), National Institute of Advanced Industrial Science and Technology (AIST), Tsukuba 305-8562, Japan*

[2]*Spin Superstructure Project (SSS), ERATO, Japan Science and Technology Corporation (JST), C/O AIST, Tsukuba 305-8562, Japan*

[3]*Institute of Multidisciplinary Research for Advanced Materials, Tohoku University, Sendai 980-8577, Japan*

[4]*Department of Applied Physics, University of Tokyo, Tokyo 113-8656, Japan*

(Received 12 April 2006; published 12 July 2006)

We have investigated the electron- and hole-doping effects on the charge-orbital order in the ordered-perovskite manganite, $EuBaMn_2O_6$. In the electron-doping case of $Eu(Ba_{1-y}La_y)Mn_2O_6$, the stacking manner of the commensurate charge-orbital ordered (CO-OO) sheets is variable between *AABB* and *ABAB* types, because of the competition between Jahn-Teller distortion and Coulomb interaction energies arising from Eu/Ba cation ordering. In the hole-doping case of $(Eu_{1-x}Ca_x)BaMn_2O_6$, on the other hand, the switching of the stacking pattern of the incommensurate CO-OO sheets does not occur, and the stacking pattern is perhaps identical with that of conventional solid-solution manganites (*AAAA* type).

DOI: 10.1103/PhysRevB.74.012402 PACS number(s): 75.47.Lx, 71.30.+h, 74.62.Bf, 75.47.Gk

Manganese oxides with perovskite structure have been attracting much attention because of the colossal magnetoresistance (CMR) effect.[1,2] The CMR effect arises from the close interplay among the charge, spin and orbital degrees of freedom, and the competition between the concomitantly charge-ordered (CO) and orbital-ordered (OO) insulator and the ferromagnetic metal (FM) state is one of the key ingredients of the CMR physics. The CO-OO state is dominant in manganites with narrow bandwidth and small disorder such as $La_{1-x}Ca_xMnO_3$ ($x \geq 0.5$) (LCMO) and $Pr_{1-x}Ca_xMnO_3$.[3,4] However, these manganites intrinsically contain considerable randomness due to the solid-solution of the perovskite *A*-site cations, which tends to make the charge-spin-orbital correlation short-ranged. The detailed study on the CO-OO phase of manganites free from such a randomness advances understanding of the CMR physics.

The *A*-site ordered manganite $LnBaMn_2O_6$ (Ln=rare earth and Y) is one of randomness-free perovskites suitable for such a study. As seen from the chemical composition, $LnBaMn_2O_6$ is a half-doped manganite, and the crystal structure consists of the alternate stacking of LnO and BaO layers to form the $2a_p$ periodicity (a_p being the cell parameter of the cubic perovskite) along the *c* axis [Fig. 1(a)].[5] In $LnBaMn_2O_6$ with Ln=Y and Sm-Dy, the *A*-site cation ordering stabilizes the CO-OO structure with high charge-orbital ordering transition temperature (T_{CO}) of 380–500 K, and gives rise to the unconventional charge-orbital order.[6–12] The *ab* plane of $LnBaMn_2O_6$ shows the checkerboard-type charge and stripe-type orbital order, identical with that often observed in conventional half-doped manganites, such as $La_{1/2}Ca_{1/2}MnO_3$ and $Pr_{1/2}Ca_{1/2}MnO_3$.[13–15] However, the stacking pattern of the CO-OO planes of $LnBaMn_2O_6$ is quite different from that of conventional manganites. In the alternate stacking of LnO and BaO layers, the CO-OO sheets stack along the *c* axis to form the $4a_p$ periodicity [*AABB* type: the left panel of Fig. 2(a)] at room temperature (RT), and the stacking manner changes from the *AABB* to *ABAB* type [the center panel of Fig. 2(a)] below T_{CO2}. It is considered that the unconventional charge-orbital order originates in the competition between Jahn-Teller (JT) distortion and Coulomb interaction energies, which is veiled by randomness in *A*-site disordered manganites. In this paper, we report the electron- as well as hole-doping effect of the *A*-site ordered manganite $EuBaMn_2O_6$ (EBMO). $Ba^{2+}(Eu^{3+})$ is replaced by $La^{3+}(Ca^{2+})$ as the electron (hole) source. The ionic radius of $La^{3+}(Ca^{2+})$ is relatively close to that of $Ba^{2+}(Eu^{3+})$. Thus it can be expected that $La^{3+}(Ca^{2+})$ preferably occupies the Ba(Eu) site so as to hold the *A*-site ordered structure.

$Eu(Ba_{1-y}La_y)Mn_2O_6$ (EBLMO) and $(Eu_{1-x}Ca_x)BaMn_2O_6$ (ECBMO) were prepared by a solid state reaction in polycrystalline form. The detailed procedure of the sample preparation was the same as that described elsewhere.[7] Synthesized samples were characterized by a powder x-ray diffraction method. Superlattice peak (0 0 1/2) in the pseudocubic setting, $a_p \times a_p \times a_p$, due to *A*-site cation ordering was clearly seen in x-ray diffraction patterns of all the prepared samples. Their crystal structures show large tetragonal or orthorhombic distortion, which provides another evidence that the degree of the *A*-site order is nearly perfect.[16] It is worth noting that melt grown samples of EBLMO and ECBMO have the simple cubic perovskite structure with complete disorder of the *A*-site cation. For these reasons, we conclude that most of $La^{3+}(Ca^{2+})$ preferably occupies Ba(Eu)-site as we expected. Transmission electron microscopy (TEM) experiments were performed with a Hitachi HF-3000S operating at 300 kV. The *A*-site cation order was also confirmed by TEM experiments. In this paper, we use the pseudo-tetragonal or pseudo-orthorhombic notation, $a_p \times a_p \times 2a_p$, to index the observed peaks in the electron-diffraction patterns (EDPs). The ac magnetization was measured with a Quantum Design Physical Property Measuring System. Differential scanning calorimetry (DSC) measurement was performed with a Seiko DSC220C.

Figures 1(b)–1(e) show the [001]-zone EDPs of EBLMO and ECBMO at 290 K. In all the EDPs, superlattice spots

 ©2006 The American Physical Society

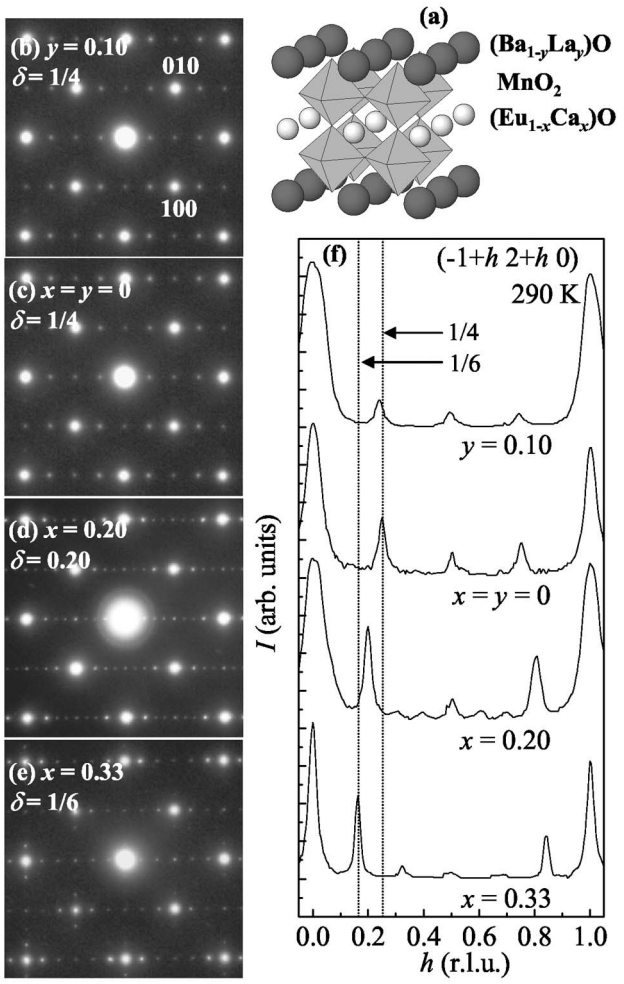

FIG. 1. (a) Schematic crystal structure of $Eu(Ba_{1-y}La_y)Mn_2O_6/(Eu_{1-x}Ca_x)BaMn_2O_6$. (b)–(e) The [001]-zone electron-diffraction patterns (EDPs) of $Eu(Ba_{1-y}La_y)Mn_2O_6$ and $(Eu_{1-x}Ca_x)BaMn_2O_6$ with $y=0.10$, $x=y=0$, $x=0.20$, and $x=0.33$, respectively, at 290 K. (f) Intensity profiles of the EDPs in (b)–(e), scanned along $(-1+h\ 2+h\ 0)$.

along the diagonal ([110]) direction are discerned clearly. These superlattice peaks come from the periodic arrangement of the charge-orbital stripe characterized by a set of modulation wave vectors $\boldsymbol{q}=(\delta,\delta,0)$. Here, δ corresponds to the inverse of the period of the orbital stripe. We show in Fig. 1(f) the intensity profiles of the EDPs in Figs. 1(b)–1(e) scanned along the [110] direction. As seen in Fig. 1(f), y/x (electron/hole-doping) dependencies of δ are quite different from each other. For the parent material EBMO (i.e., $x=y=0$), δ takes a commensurate value of 1/4, evidencing the four-times periodicity of the orbital stripe along the diagonal direction.[8–12] The value of δ of EBLMO ($y=0.10$) is the same as that of $x=y=0$, indicating that the $\delta=1/4$ CO-OO structure is robust against electron-doping. In contrast, δ of ECBMO depends on Ca concentration x; $\delta=0.20$ at $x=0.20$ and $\delta=0.16$ at $x=0.33$. The y/x dependencies of δ and the electronic phase diagram for EBLMO and ECBMO are shown in Figs. 2(b) and 2(c), respectively. The δ value shows conspicuous electron-hole asymmetry: In the La(electron)-doped region, δ keeps the commensurate value with variation of y, whereas in the Ca(hole)-doped region, δ is incommensurate and linearly depends on Ca concentration x. Such a linear dependence of δ is observed also in conventional manganites such as LCMO ($x\geq 0.5$).[3]

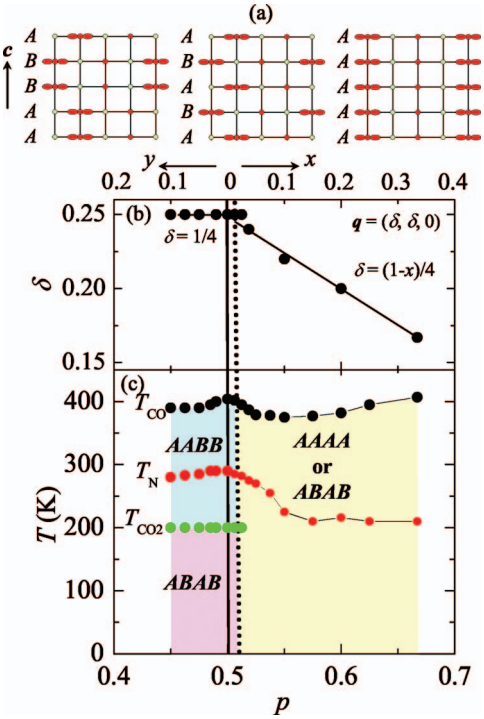

FIG. 2. (Color) (a) Schematic charge-orbital ordered (CO-OO) structures viewed in the bc plane. Green circles represent Mn^{4+}, and red circles and lobes represent Mn^{3+} with $3x^2-r^2$ and $3y^2-r^2$ orbitals, respectively. (b) The y and x dependence of δ in the modulation vector $(\delta,\delta,0)$, and (c) the electronic phase diagram for $Eu(Ba_{1-y}La_y)Mn_2O_6$ and $(Eu_{1-x}Ca_x)BaMn_2O_6$, respectively. The abscissa represents the total hole-doping level $p=(1+x-y)/2$. T_{CO}, T_{CO2}, and T_N denote the charge-orbital ordering, switching of the CO-OO structure, and antiferromagnetic transition temperatures, respectively.

Figure 3 shows the temperature dependence of the ac magnetizations for $x=y=0$ and $y=0.10$ measured with the 10 kHz ac magnetic field ($h=1$ Oe). For the parent state ($x=y=0$), the in-phase [M', Fig. 3(a)] and out-of phase components [M'', 3(b)] show an anomaly around 290 K, corresponding to the antiferromagnetic transition temperature (T_N). The anomaly of M' around $T_{CO2}=200$ K is ascribed to the switching of the CO-OO stacking structure.[8,10–12] The net moment below T_N abruptly evolves with electron-doping y, and M'' for $y=0.10$ shows a slight anomaly around 200 K. The temperature dependence of electron-diffraction intensity profiles along $(3/2\ 1/2\ l)$ is exhibited for $y=0.10$ in the inset of Fig. 3(a). The superlattice peak at $l=0.5$ is clearly seen in the profiles at 290 and 220 K but disappears at and below 200 K, where the anomaly of M'' is observed. This coincidence proves that the stacking manner of the CO-OO sheet changes from the $AABB$ to $ABAB$ type around $T_{CO2}=200$ K just as in the case of $x=y=0$. The DSC curves of $x=y=0$ and $y=0.10$ are shown in the inset of Fig. 3(b). The

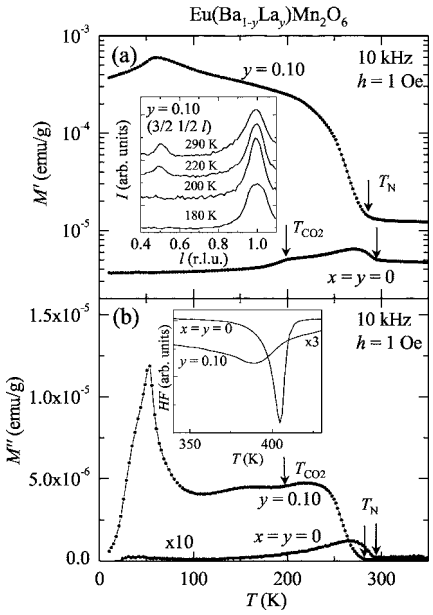

FIG. 3. Temperature dependence of the (a) in-phase (M') and (b) out-of-phase (M'') components of the ac magnetizations for $y=0$ and $y=0.10$ of $Eu(Ba_{1-y}La_y)Mn_2O_6$, measured with the amplitude $h=1$ Oe of applied field. Insets in (a) and (b) show intensity profiles of EDPs for $y=0.10$ scanned along (3/2 1/2 l) and differential scanning calorimetry (DSC) curves of $y=0$ and $y=0.10$, respectively. The ordinate of the inset in (b) represents the heat flow (HF).

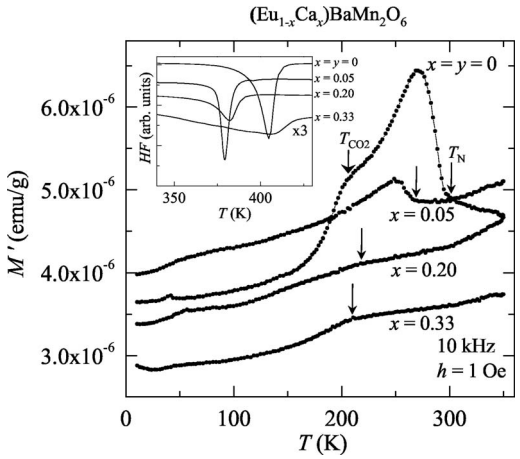

FIG. 4. Temperature dependence of the in-phase component of the ac magnetizations (M') for $x=0$, 0.05, 0.20 and 0.33 of $(Eu_{1-x}Ca_x)BaMn_2O_6$. The inset shows differential scanning calorimetry (DSC) curves of the respective samples.

strong endothermic peak around 400 K for $x=y=0$ is attributed to the charge-orbital ordering transition. T_{CO} for $y=0.10$ slightly shifts to lower temperature of 395 K, and the transition is rather diffusive compared with that for $x=y=0$.

Let us proceed to the Ca-doping (hole-doping) case. As shown in Fig. 2(b), in contrast to the La-doping case, δ depends on the Ca concentration x, obeying the relation that $\delta=(1-x)/4$. At $x=0.33$, δ takes another commensurate value of 1/6, implying that the Mn^{3+} stripes are arranged as far apart from each other as possible to form the six-times periodicity.[3,17,18] Temperature dependence of the ac magnetization for ECBMO is shown in Fig. 4. With increasing Ca concentration x, contrary to the La-doping (electron-doping) case, the net moment below T_N is suppressed, and T_N gradually shifts to lower temperature. The anomaly at T_{CO2} totally vanishes even in the minimally Ca-doped compound ($x=0.05$). No superlattice spot along the c^* axis can be observed in any EDPs of ECBMO at 290 and 77 K, indicating that the switching of the CO-OO structure as observed in the parent EBMO does not occur. The DSC curves of ECBMO are shown in the inset of Fig. 4. T_{CO} slightly decreases with the increase of x, taking the minimum value of 380 K at $x=0.10$. Then, T_{CO} is increased again by further Ca doping, finally reaching 410 K at $x=0.33$.

We have summarized the present results as the y and x dependence of δ [Fig. 2(b)] and the electronic phase diagram for EBLMO and ECBMO [Fig. 2(c)]. For the abscissa of Fig. 2(c) is taken, the total hole-doping level $p=(1+x-y)/2$ from the Mn^{3+} based compound. In the electron-doped region, δ is independent of La concentration y, taking always the commensurate value of 1/4, whereas in the hole-doped region, δ is incommensurate and varies as $\delta=(1-x)/4$. The commensurate and incommensurate regions are separated by a first-order-transition line at $x=y=0$ (EBMO), and the stacking manners of the CO-OO sheets in the both regions are different from each other. The electron-hole asymmetry of the CO-OO structure in the ab plane is attributed perhaps to the interaction between the adjacent orbital stripes of Mn^{3+}. In the case of EBLMO, the $\delta=1/4$ CO-OO structure is very robust, and doped excess electrons randomly occupy the Mn^{4+} stripes. Consequently, δ is constant in EBLMO. Evolution of the weak ferromagnetism by La doping may come from double-exchange mechanism mediated by excess electrons on the Mn^{4+} sites.[19–21] In the Ca-doped region, on the other hand, the orbital stripes of Mn^{3+} are as far apart from each other as possible to reduce JT distortion and Coulomb repulsion energies between the orbital stripes. As a result, the linear x dependence of δ is observed. Similar asymmetric charge-orbital order is also observed in conventional manganites with narrow bandwidth and small disorder such as PCMO.[22,23] A significant difference between the A-site ordered and disordered (solid-solution) manganites is in the stability of the CO-OO state and the stacking manner of the CO-OO sheets as argued in the following.

In the case of Ln (Y and Sm-Dy) with a smaller ionic radius, the large mismatch between the ionic radii of Ln and Ba probably enhances uniform JT distortion in the A-site ordered structure to stabilize the orbital order accompanied with the charge order. With the increase of La(Ca) doping, random Coulomb potential in $(Ba_{1-y}La_y)O((Eu_{1-x}Ca_x)O)$ layer may be increased even in the nominally ordered structure. Nevertheless the CO-OO state is still robust, and moreover T_{CO} for $x=0.33$ is still comparable to that for $x=y=0$. On the other hand, all the A-site solid-solution compounds of EBLMO and ECBMO are spin-glass insulators with no long-range charge-orbital order. These results imply a more important role of the inhomogeneous local lattice distortion, rather than the Coulomb potential randomness, in destabilizing the long-range charge-orbital order, or the regular array of JT-distorted $Mn^{3+}O_6$ octahedra.

Another feature arising from *A*-site cation ordering is the unconventional stacking manner of the CO-OO sheets and its temperature- and doping-dependent switching, which are ascribed to the competition between JT distortion and Coulomb interaction energies. As mentioned above, the switching of the CO-OO structure occurs in EBMO and EBLMO, while not in ECBMO. In EBMO and EBLMO, the *ABAB* type stacking, that is, NaCl-type charge order is realized as the ground state to minimize Coulomb potential energy. In ECBMO, by contrast, no superlattice peak assigned to $(n/2\ m/2\ k/2)$ (n, m and k being odd numbers) are observed in EDPs. There are two possible models for the stacking manner to account for the disappearance or absence of the superlattice peak, as observed for EBMO ($x=y=0$) and EBLMO ($y=0.10$) below T_{CO2}. One is the *ABAB* type stacking [center panel of Fig. 2(a)]. The other is the *AAAA* type [right panel of 2(a)], as observed for *A*-site solid-solution manganites. This *AAAA* type stacking may favor the collective JT distortion of $Mn^{3+}O_6$, rather than the *ABAB* type one. In the Ca-doped region, the decrease of e_g-electron number from half-doping level probably weakens the effect of Coulomb term, and consequently JT-distortion energy determines the stacking pattern of the CO-OO sheets, i.e., the *AAAA* type stacking.

In summary, we have investigated the electron- and hole-doping effects on the CO-OO state in the *A*-site ordered manganite, $EuBaMn_2O_6$, in which Ba^{2+} and Eu^{3+} are partially substituted with La^{3+} and Ca^{2+}, respectively. The commensurate and incommensurate CO-OO regions are separated by a first-order-transition line locating at $EuBaMn_2O_6$. In $EuBaMn_2O_6$ and La(electron)-doped analogs, the stacking manner of the $\delta=1/4$ CO-OO sheets is variable between the *AABB* and *ABAB* types, perhaps because of subtle balance between Jahn-Teller distortion and Coulomb interaction energies. On the other hand, in the Ca(hole)-doped case, JT-distortion energy appears dominant over Coulomb interaction energy, and the stacking pattern of the incommensurate CO-OO sheets does not change, perhaps maintaining the *AAAA* type.

We would like to thank H. Takagi, N. Nagaosa, and R. Mathieu for valuable discussions. This work was partly supported by New Energy and Industrial Technology Development Organization (NEDO) and by a Grant-In-Aid for Scientific Research from the MEXT of Japan.

*Present address: Department of Physics, Sophia University, Tokyo 102-8554, Japan. Electronic address: d-akahos@sophia.ac.jp

[1] E. Dagotto, T. Hotta, and A. Moreo, Phys. Rep. **344**, 1 (2001).
[2] Y. Tokura, Rep. Prog. Phys. **69**, 797 (2006).
[3] C. H. Chen, S.-W. Cheong, and H. Y. Hwang, J. Appl. Phys. **81**, 4326 (1997).
[4] Y. Tomioka, A. Asamitsu, H. Kuwahara, Y. Moritomo, and Y. Tokura, Phys. Rev. B **53**, R1689 (1996).
[5] F. Millange, V. Caignaert, B. Domengès, B. Raveau, and E. Suard, Chem. Mater. **10**, 1974 (1998).
[6] T. Nakajima, H. Kageyama, H. Yoshizawa, and Y. Ueda, J. Phys. Soc. Jpn. **71**, 2843 (2002).
[7] D. Akahoshi, M. Uchida, Y. Tomioka, T. Arima, Y. Matsui, and Y. Tokura, Phys. Rev. Lett. **90**, 177203 (2003).
[8] T. Arima, D. Akahoshi, K. Oikawa, T. Kamiyama, M. Uchida, Y. Matsui, and Y. Tokura, Phys. Rev. B **66**, 140408(R) (2002).
[9] M. Uchida, D. Akahoshi, R. Kumai, Y. Tomioka, T. Arima, Y. Tokura, and Y. Matsui, J. Phys. Soc. Jpn. **71**, 2605 (2002).
[10] H. Kageyama, T. Nakajima, M. Ichihara, Y. Ueda, H. Yoshizawa, and K. Ohoyama, J. Phys. Soc. Jpn. **72**, 241 (2003).
[11] T. Nakajima, H. Kageyama, M. Ichihara, K. Ohoyama, H. Yoshizawa, and Y. Ueda, J. Solid State Chem. **177**, 987 (2004).
[12] D. Akahoshi, Y. Okimoto, M. Kubota, R. Kumai, T. Arima, Y. Tomioka, and Y. Tokura, Phys. Rev. B **70**, 064418 (2004).
[13] E. O. Wollan and W. C. Koehler, Phys. Rev. **100**, 545 (1955).
[14] P. G. Radaelli, D. E. Cox, M. Marezio, and S.-W. Cheong, Phys. Rev. B **55**, 3015 (1997).
[15] Z. Jirak, S. Krupicka, Z. Simsa, M. Dlouha, and S. Vratislav, J. Magn. Magn. Mater. **53**, 153 (1985).
[16] T. Nakajima, H. Yoshizawa, and Y. Ueda, J. Phys. Soc. Jpn. **73**, 2283 (2004).
[17] M. T. Fernández-Díaz, J. L. Martínez, J. M. Alonso, and E. Herrero, Phys. Rev. B **59**, 1277 (1999).
[18] P. G. Radaelli, D. E. Cox, L. Capogna, S.-W. Cheong, and M. Marezio, Phys. Rev. B **59**, 14440 (1999).
[19] C. Zener, Phys. Rev. **82**, 403 (1951).
[20] P. W. Anderson and H. Hasegawa, Phys. Rev. **100**, 675 (1955).
[21] P.-G. de Gennes, Phys. Rev. **118**, 141 (1960).
[22] C. H. Chen, S. Mori, and S.-W. Cheong, Phys. Rev. Lett. **83**, 4792 (1999).
[23] M. v. Zimmermann, C. S. Nelson, J. P. Hill, Doon Gibbs, M. Blume, D. Casa, B. Keimer, Y. Murakami, C.-C. Kao, C. Venkataraman, T. Gog, Y. Tomioka, and Y. Tokura, Phys. Rev. B **64**, 195133 (2001).